# ARTICLES

## Formamide in Reverse Micelles: Restricted Environment Effects on Molecular Motion

**Ruth E. Riter, Erik P. Undiks, Joel R. Kimmel, and Nancy E. Levinger***

*Department of Chemistry, Colorado State University, Fort Collins, Colorado 80523-1872*

*Received: February 11, 1998; In Final Form: June 19, 1998*

Novel Aerosol OT (AOT) reverse micelles solubilizing formamide rather than water have been created and studied. In contrast to water sequestered in the interior of AOT reverse micelles, the vibrational spectra indicate that the intramicellar formamide retains a large degree of hydrogen bonding character and its structure appears significantly less perturbed by the restricted environment than water. However, solvation dynamics measurements show that the intramicellar formamide is nearly completely immobilized, a dramatic departure from bulk solvation dynamics. These results show that structural aspects derived from the characteristic vibrational motion does not necessarily provide insight into other dynamical solvent behavior.

### I. Introduction

There exists a wide range of chemical processes that occurs in heterogeneous rather than homogeneous solutions. In particular, organized media such as micelles and vesicles can provide inhomogeneous environments for specialized chemistry. When surfactant molecules are dissolved in nonpolar solvents, self-assembly to reverse micelles can occur. These structures serve well as microreactors for heterogeneous chemistry,[1] as templates for nanoparticles,[1,2] and as mimics for biological membranes.[1] The chemistry occurring in these reverse micelles depends in part on the nature of the water inside the micelles.

While many surfactants have been used to form reverse micelles, the most common systems probed employ the surfactant Aerosol OT (AOT).[2] The molecular structure for AOT is shown in Figure 1. Both structural and dynamical aspects of the AOT reverse micelles and the water solubilized within them have been explored. AOT micelles have been shown to form spherical droplets the radii of which are directly proportional to the molar ratio of water to surfactant,[3]

$$w_0 = \frac{[H_2O]}{[AOT]} \tag{1}$$

AOT reverse micelles are reported to form in a wide variety of nonpolar phases including alkane, halocarbon, and aromatic solvents.[2]

One method that has been used to characterize the AOT reverse micelles is vibrational spectroscopy.[4−11] From spectral shifting of bands in IR and Raman spectra, researchers have described the intramicellar water having two different forms: molecules that interact strongly with the surfactant polar headgroups, or bound water, and water that appears to possess similar hydrogen-bonding characteristics to the bulk phase, or free water. This is evident both from studies of the water vibrational modes and from the AOT functional group modes, such as the sulfonate and carbonyl. The relative contribution from these two water types depends on the amount of water solubilized within the micelles. For low water loading, all the water inside exists in the bound form. As the water content is increased, bulklike hydrogen bonding characteristics appear, eventually dominating the spectrum.

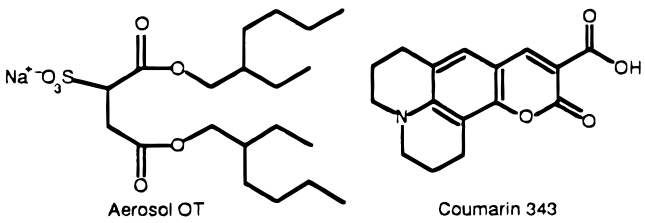


**Figure 1.** Molecular structure for the surfactant aerosol OT and the molecular probe coumarin 343.

Dynamical measurements have also been used to characterize the intramicellar water.[12−18] These studies all find that the water inside the micelles moves differently from bulk water. Using viscosity sensitive probes, Hasegawa et al. have measured the microviscosity inside reverse micelles of varying size.[12] Their results indicate that the water inside micelles with $w_0 < 10$ has a higher viscosity than that of the bulk they ascribe to water bound to the AOT polar headgroups. For micelles larger than $w_0 = 10$, the viscosity decreases slowly as the micellar size increases. Zhang and Bright[13] and Cho et al.[14] have explored solvent relaxation via fluorescence properties of the molecular probe 1,8-anilino-8-naphthalenesulfonic acid. Their results reveal two different solvation rates inside the micelles that they attribute to water bound to the polar headgroups of AOT and bulklike water in the micelles. Via the time-resolved fluorescence of coumarin 480 in heptane/AOT/water reverse micelles, Sarkar et al.[15] measured nanosecond components of the water solvation motion. In general, the results from all these studies indicate that water in AOT reverse micelles moves more slowly than bulk water. However, for all these studies, the experimental time resolution was insufficient to measure motion of bulk water that occurs on an ultrafast, sub-picosecond time scale.[19]

* Corresponding author. E-mail: levinger@lamar.colostate.edu.

S1089-5647(98)01058-X CCC: $15.00 © 1998 American Chemical Society
Published on Web 09/23/1998

Recently, the ultrafast solvation dynamics of water in AOT reverse micelles have been explored.[16−18] Solvation dynamics follows the response of solvent molecules to an instantaneous electric perturbation.[20−22] The motions responsible for solvation dynamics are primarily rotational and translational. The solvation dynamics in bulk solution have been studied in detail[23−25] revealing two different responses, inertial and diffusive, that occur on different time scales and arise from different types of solvent motion. Solvation dynamics studies have been extended to heterogeneous environments including reverse micelles,[15−18] surfaces[26,27] and cyclodextrin cavities.[28] We have used ultrafast fluorescence upconversion spectroscopy of coumarin 343 (C343) in water/AOT/isooctane reverse micelles to follow water motion.[16,17] These experiments showed that water motion in the smallest micelles was essentially frozen while in larger micelles additional bulklike relaxation components developed. Mittleman et al. have also investigated water motion on an ultrafast time scale using time-resolved optical Kerr effect measurements.[18] Their results showed that the amplitude of the water motion was substantially reduced in the micelles. On the basis of the differences of the water inside small and large reverse micelles, it is not surprising that the dynamics also differ dramatically.

In comparison with the extensive information available about water in AOT reverse micelles, there are only a few references to reverse microemulsions[29] where the polar phase is anything other than water.[30−43] And, while the water sequestered in reverse micelles has been well characterized via a plethora of experimental techniques,[2,4−10,44] the properties of other polar solvents present in reverse microemulsions are relatively unknown. Recently, we have begun probing the formation of AOT reverse micelles solubilizing nonaqueous polar solvents.[30]

One alternative polar solvent that forms reverse micelles is formamide.[30−35] Formamide is an interesting solvent because in bulk liquid it develops an extended hydrogen-bonded structure. This hydrogen bonding is evident in the formamide IR spectrum from both the $NH_2$ and C═O vibrational modes that shift $=100$ cm$^{-1}$ from higher to lower frequencies concurrent with the onset of hydrogen bonding.[45−49] Therefore, the vibrational frequencies of the $NH_2$ and C═O modes are accurate indicators of the local environment of the formamide molecules. These vibrational modes have been used in various studies to reveal changes in the liquid structure, for example, when formamide is mixed with other solvents or electrolytes.[50−52]

Solvation dynamics of bulk formamide have been explored.[23,53,54] While it shares extensive hydrogen bonding characteristics with water, the solvation dynamics of formamide are significantly slower. In particular, the inertial component of the solvation dynamics that comprises more than 50% of the water response[19] represents a mere 10% of the relaxation observed in formamide.[23] The diffusive components of the formamide solvation dynamics are also slower than those for water.

In the work reported here, we probe the vibrations of deuterated formamide solubilized in Aerosol OT reverse micelles using IR spectroscopy and the solvation dynamics of formamide within the micelles using ultrafast time-resolved fluorescence measurements. We make direct comparisons between the vibrational spectroscopy and solvation dynamics of formamide in reverse micelles with water and $D_2O$ in reverse micelles. We also compare our results to the vibrational spectroscopy and solvation dynamics of bulk formamide to show how the sequestered formamide environment differs inside the micelles. We find that the structural features indicated by the vibrational spectra do not provide insight about dynamical rotational and translational properties of the intramicellar formamide indicated from the solvation dynamics.

**TABLE 1: Micellar Radii Measured with Dynamic Light Scattering**

| reverse micelle | $w_{FA}$ | radius (nm) |
|---|---|---|
| formamide/AOT/$CCl_4$ | 1.1 | $4.5 \pm 1.4$[a] |
| formamide/AOT/isooctane | 1.1 | $3.5 \pm 0.5$ |

[a] The refractive index of formamide and $CCl_4$ are very similar.[68] Therefore, the intensity of the scattered light from the micelles is extremely low leading to a large uncertainty for the measurement.

## II. Materials and Methods

**Sample Preparation**. Aerosol OT (sodium bis(2-ethylhexyl)-sulfosuccinate, Aldrich) was thoroughly dried over molecular sieves (Sigma, 3 Å) in ether. The ether was removed under vacuum. All subsequent handling was performed in an $N_2$ atmosphere. A Karl-Fisher titration of the AOT showed less than 0.15% water corresponding to 0.037 water molecules per AOT molecule.[55] The highest grade formamide (FA, HPLC grade, Aldrich) was used without further purification. Deuteration of the FA was effected by mixing a 10:1 solution of $D_2O$ (Cambridge Isotopes) with the FA, stirring the mixture for several days, and then boiling off the $D_2O$ at 110 °C. We estimate >90% H−D exchange based on the absence of $NH_2$ bands in the IR spectrum. Coumarin 343, shown in Figure 1, was purchased from Exciton and used as received.

Reverse micelles were created by first dissolving the dry AOT in carbon tetrachloride (HPLC grade, Aldrich) or isooctane (2,2,4-trimethylpentane, HPLC grade, Aldrich) to which was added the requisite amount of FA or deuterated formamide ($d_2$−FA) or $D_2O$. All samples displayed a single isotropic phase that appeared clear by eye for all the concentrations probed. We refer to the samples based on the relative amount of FA compared to AOT, that is,

$$w_{FA} = \frac{[FA]}{[AOT]} \tag{2}$$

as is commonly done for aqueous reverse microemulsions.[2] In addition, the volume fraction of surfactant and polar solvent in the solution,

$$\phi = \frac{V_{FA} + V_S c v_s}{V_{TOT}} \tag{3}$$

was kept below 10%. Here $V_{FA}$ is the volume of normal or deuterated FA, $V_S$ is the volume of a stock solution of AOT in nonpolar solvent, $c$ is the concentration of the stock solution, $v_S$ is the AOT molar volume (0.391 l/mol),[56] and $V_{TOT}$ is the volume of the entire solution. This ensured that the samples contained reverse micelles rather than another extended microstructure.

The size of the reverse micelles was determined with dynamic light scattering (DynaPro-MSTC, protein solutions). The micellar radii are given in Table 1.

**Infrared Spectra.** Infrared vibrational spectra were collected with an FTIR Spectrophotometer (Nicolet, Magna 760). Individual spectra represent averages of 128 scans with 8 cm$^{-1}$ resolution. Higher resolution scans revealed no additional features or spectral narrowing indicating that the spectral features observed for lower resolution scans result from the sample environment and not from the FTIR instrument. Samples were

introduced either in an IR microvolume $CaF_2$ cuvette or on $CaF_2$ plates. The optical properties of the $CaF_2$ material limited our spectra to frequencies above ~1400 $cm^{-1}$. Unfortunately, this precluded measurements of the AOT sulfonate vibrational modes. Spectra were base line subtracted and were normalized using the $CH_2$ stretch region of the AOT spectrum to achieve relative intensities for the $d_2$−FA and $D_2O$ contributions.

**Solvation Dynamics Measurements.** The time-resolved fluorescence upconversion apparatus has been described in detail elsewhere.[16] Briefly, we use the doubled output from an ultrafast mode-locked Ti:sapphire laser at 410 nm to excite the dye to its first excited state. The resulting fluorescence is mixed with the residual laser fundamental gate pulse in a nonlinear BBO crystal a variable time later thereby time-resolving the fluorescence. The time resolution of the spectrometer, determined via cross-correlation of the excitation and gate pulses in the nonlinear crystal, is <170 fs, assuming a Gaussian profile. The upconverted fluorescence is dispersed with a prism and sent through a monochromator where it is detected with a cooled PMT. The bandwidth of the sum-frequency radiation collected is 8 nm. Signals are collected via a photon counter interfaced to a computer. The time-resolved fluorescence signals are averaged over 4−8 individual scans and are collected over a ~100 nm range in 10 nm steps. Each fluorescence decay is fit to a multiexponential function using a Global variable fit function. Transient fluorescence spectra are reconstructed from the fluorescence decays. The normalized time-correlation function,

$$C(t) = \frac{\nu(t) - \nu(\infty)}{\nu(0) - \nu(\infty)} \quad (4)$$

and the unnormalized time-correlation function,

$$S(t) = \nu(0) - \nu(t) \quad (5)$$

are generated from the transient fluorescence spectra, where $\nu$(t), $\nu$(0), and $\nu$(∞) are the peak of a log-normal function fit to the reconstructed fluorescence spectra at time t, 0, and at equilibrium, respectively. $C(t)$ functions are used to determine the dynamics, while $S(t)$ functions are used to compare overall Stokes shifts and dynamics concurrently.

Absorption and emission spectra of the C343 probe molecule were characterized prior to the dynamical measurements. Absorption spectra were obtained with a Cary 2400 UV−vis−IR spectrophotometer. Emission spectra were measured with a home-built fluorometer.[57] Time-correlated single-photon counting (TCSPC) was used to measure the fluorescence lifetime of the C343 probe molecule in the various milieus.[58] All experiments were carried out at room temperature, 21 ± 2 °C.

## III. Results

**Vibrational Spectra.** The IR spectra of bulk $d_2$−FA, $d_2$−FA, and $D_2O$ solubilized in AOT reverse micelles in $CCl_4$, and dry AOT dissolved in $CCl_4$ are shown in Figure 2. We have chosen to examine $d_2$−FA rather than protonated FA in these studies, because the $NH_2$ stretching region of the protonated FA spectrum, appearing near 3400 $cm^{-1}$, is complicated by a resonance with the overtone of another vibrational mode.[59] This Fermi resonance is not present in the spectrum of the deuterated compound, making spectral deconvolution and assignment more straightforward. Carbon tetrachloride was chosen over isooctane for the IR spectra because it allowed us to normalize the spectra to the AOT $CH_2/CH_3$ stretching modes thus compare spectral peak intensity as well as position. Furthermore, it was impossible to cleanly subtract the overwhelming background observed for spectra obtained in hydrocarbon solvents. The spectra in Figure 2 are shown from 1600 to 3000 $cm^{-1}$, a frequency range spanning the C═O stretch to the CH stretches. No features are observed at higher frequencies indicating imperceptible water or protonated FA in the samples. Figures 3 and 4 show expanded portions of the spectra focusing on the $ND_2$ and OD symmetric and antisymmetric stretch (2200−2700 $cm^{-1}$), and the C═O stretch (1600−1800 $cm^{-1}$) regions, respectively. Spectra for protonated FA/AOT/$CCl_4$ reverse micelles were also examined and follow similar, if not identical trends as the $d_2$−FA spectra.

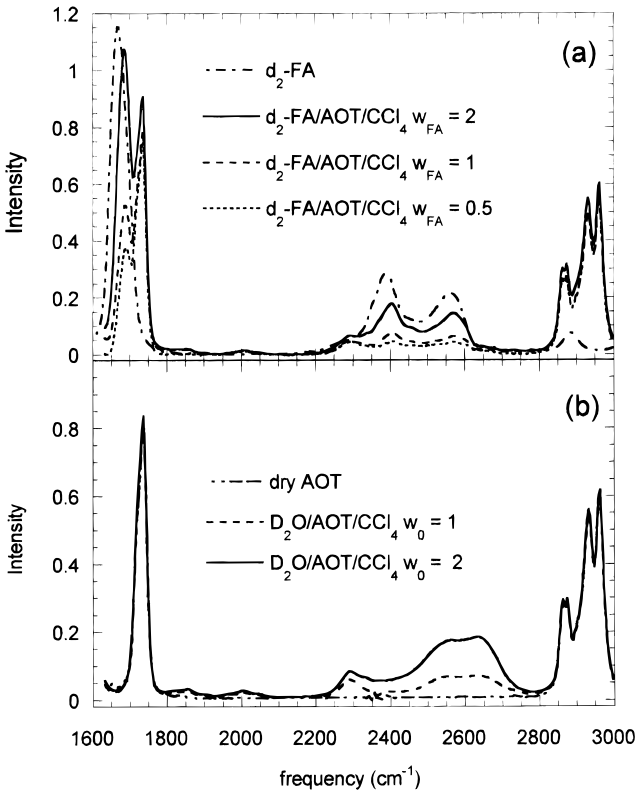


**Figure 2.** Infrared spectra of (a) deuterated formamide in aerosol OT reverse micelles in $CCl_4$, (b) $D_2O$ aerosol OT reverse micelles in $CCl_4$ and dry AOT in $CCl_4$.

The $ND_2$ stretching region of $d_2$−FA spectra in the AOT reverse micelles is shown in Figure 3a. Frequencies for the observed bands are listed in Table 2. The IR spectrum of liquid $d_2$−FA in this frequency range is dominated by two spectral features associated with the symmetric, $\nu_s$, and antisymmetric, $\nu_a$, stretching modes, at 2385 and 2556 $cm^{-1}$, respectively.[45−47,49] Often a shoulder appears near 2450 $cm^{-1}$ in liquid samples due to the incompletely deuterated species, NHD. Our spectrum for the bulk liquid spectrum reveals the symmetric and antisymmetric stretch peaking at 2387 and 2561 $cm^{-1}$, respectively, and the 2450 $cm^{-1}$ shoulder. The spectra of $d_2$−FA in the reverse micelles reveals corresponding modes appearing at slightly higher frequencies. For example, the symmetric stretch appears at 2407 $cm^{-1}$ in the $w_{FA} = 0.5$ sample and shifts down to 2403 $cm^{-1}$ for $w_{FA} = 2.0$. The antisymmetric stretch peaks at 2574 $cm^{-1}$ for $w_{FA} = 0.5$ shifting to 2569 $cm^{-1}$ for $w_{FA} = 2.0$. The shape of the peaks remains largely unchanged between the spectra.

The spectra of $D_2O$ in the AOT reverse micelles, Figure 3b, are relatively simple. The only feature associated with OD motion appears near 2600 $cm^{-1}$ and can be deconvoluted into two frequency components, one peaking near 2550 $cm^{-1}$ and

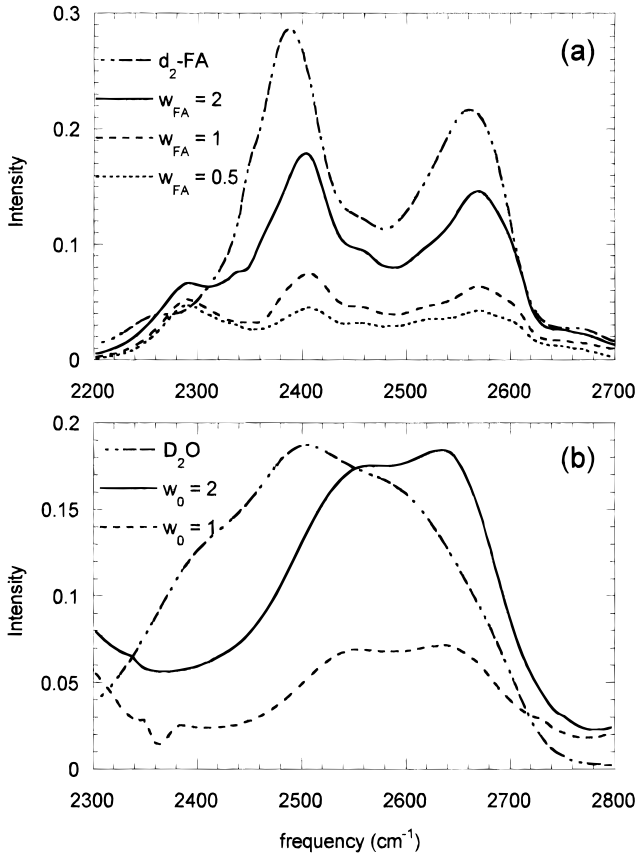


**Figure 3.** Infrared spectra of the $ND_2$ and OD stretching region of (a) bulk deuterated formamide, deuterated formamide in Aerosol OT reverse micelles in $CCl_4$, (b) bulk $D_2O$, and $D_2O$ in Aerosol OT reverse micelles in $CCl_4$.

the other near 2650 $cm^{-1}$. These components can be assigned to strongly and weakly hydrogen-bonded OD moieties, respectively.[60] This is consistent with reports in the literature.[4−9,11]

We have also examined the C═O stretching frequency of FA and AOT to learn about the environment inside the micelles. In Figure 4, the C═O stretching region is shown. Frequencies of the FA C═O stretch in the various environments are listed in Table 2. In the micelles solubilizing $D_2O$, Figure 4b, the only contribution to the spectra comes from the AOT carbonyl moieties. This band can be deconvoluted into two frequency components peaking at 1729 and 1738 $cm^{-1}$, consistent with reports in the literature.[9,10] In contrast, the micelles solubilizing $d_2$−FA reveal an additional feature due to the $d_2$−FA carbonyl group. This feature grows more intense as $w_{FA}$ increases. The frequencies of the AOT bands do not shift as either $D_2O$ or $d_2$−FA is added to the micelles. However, the vibrational frequency of the $d_2$−FA carbonyl is higher for $d_2$−FA inside the micelles than in the bulk liquid; the peak in bulk liquid $d_2$−FA appears near 1670 $cm^{-1}$ [49] while the C═O stretch peaks at 1686 $cm^{-1}$ in the micelles.

**Solvation Dynamics.** The solvation dynamics of bulk FA and FA inside AOT reverse micelles in isooctane, $w_{FA} = 1.1$, were measured via ultrafast time-resolved fluorescence upconversion. The time resolution of the upconversion instrument precluded measurement of the inertial component in the samples probed. However, ultrafast diffusive components were easily observed. The C343 probe molecule is completely insoluble in isooctane but somewhat soluble in $CCl_4$. As a result, reverse micellar solutions were investigated in isooctane rather than in $CCl_4$ to ensure that the C343 dye molecule reflected only dynamics of the solubilized polar solvent, FA, and not the

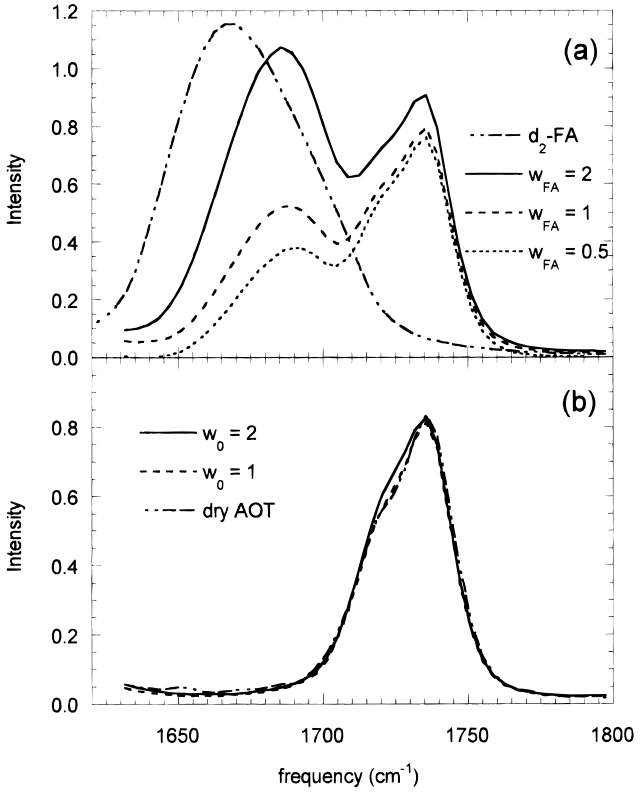


**Figure 4.** Infrared spectra of the C═O stretching region of (a) bulk deuterated formamide, deuterated formamide in Aerosol OT micelles in $CCl_4$, (b) dry Aerosol OT in $CCl_4$, and $D_2O$ in Aerosol OT reverse micelles in $CCl_4$.

**TABLE 2: Vibrational Frequencies for the $ND_2$ and C═O Stretching Modes of Deuterated Formamide Bulk Liquid and Solubilized in Aerosol OT Reverse Micelles in $CCl_4$**

| | frequency ($cm^{-1}$) | | | | |
|---|---|---|---|---|---|
| | bulk | | in reverse micelle | | |
| vibrational mode | bulk liquid[a] | Xe matrix[b] | $w_{FA}$ = 0.5 | $w_{FA}$ = 1.0 | $w_{FA}$ = 2.0 |
| $ND_2$ $\nu_a$ | 2561 | 2663 | 2574 | 2569 | 2568 |
| $ND_2$ $\nu_s$ | 2387 | 2498 | 2407 | 2405 | 2403 |
| C═O $\nu_s$ | 1668 | 1732 | 1686 | 1686 | 1686 |

[a] Literature values for these modes are 2556, 2385, and 1667 cm for the $ND_2$ $\nu_a$, $ND_2$ $\nu_s$, and C═O $\nu_s$ modes, respectively.[45] [b] Values taken from ref 47.

dynamics outside the reverse micelles. We have measured the size of the $w_{FA} = 1.1$ reverse micelles in isooctane using dynamic light scattering and found them to be very similar to the $w_{FA} = 2.0$ micelles in $CCl_4$ discussed in the preceding section, see Table 1.

The time correlation functions for FA in the micelles and in bulk are shown in Figure 5. The normalized time correlation function, C(t), for bulk FA solvation dynamics is shown in Figure 5a. This C(t) fits well to a biexponential decay with time constants equal to 0.11 and 2.4 ps, and amplitudes of 0.55 and 0.45, respectively. These time constants and amplitudes agree well with reports in the literature.[23,53,54] In contrast, C(t) for FA inside the reverse micellar sample shows significantly reduced relaxation on the time scale of the bulk dynamics. The C(t) function for C343 in the FA/AOT/isooctane reverse micelles requires a triexponential function to accurately fit. The time constants equal 0.5, 25, and 240 ps and amplitudes are 0.2, 0.2, and 0.6, respectively. A plot of the unnormalized time-correlation function S(t) in Figure 5b contrasts the amplitude

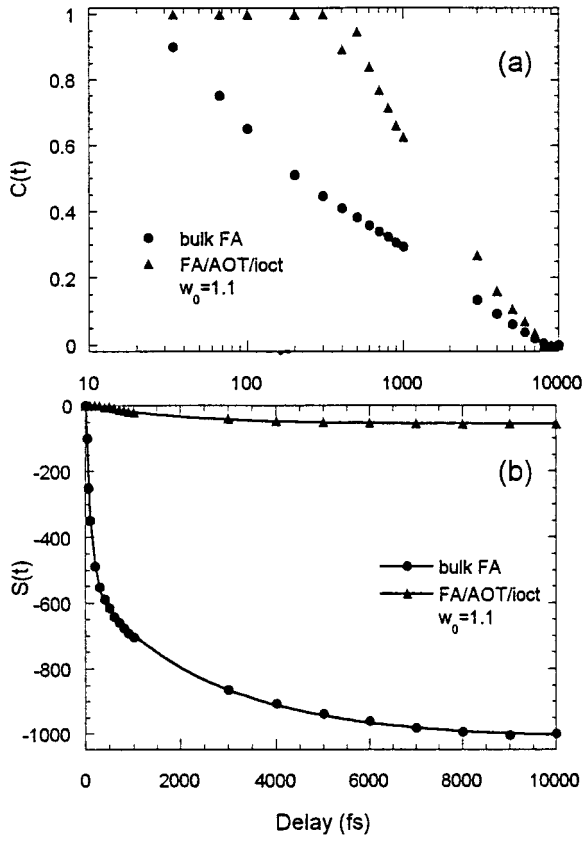


**Figure 5.** (a) Normalized time-correlation function C(t) for coumarin 343 in bulk formamide and formamide/Aerosol OT/isooctane reverse micelles. (b) Unnormalized time-correlation function S(t) for coumarin 343 in bulk formamide and formamide/Aerosol OT/isooctane reverse micelles.

of the overall Stokes shift and the time scale for motion observed. The Stokes shift in bulk FA is ~1000 $cm^{-1}$, while in the micelles it is ~50 $cm^{-1}$. The largest decay component in the reverse micelles occurs on the 100 ps time scale, substantially longer than any relaxation components of the bulk liquid.[23,53,54] TCSPC measurements showed that the lifetime of the dye is essentially the same in the micelles as it is in bulk solution.

## IV. Discussion

**Vibrational Spectra.** Several features of the $d_2$−FA IR spectra warrant discussion. First, the $ND_2$ stretching range, 2200−2700 $cm^{-1}$, of the spectra bear significant resemblance to the spectrum in bulk liquid $d_2$−FA, see Figure 3a.[45] Contributions from modes at frequencies associated with the isolated nonhydrogen bonded molecule are not observed.[47,48] The $ND_2$ symmetric and antisymmetric stretching frequencies are only modestly impacted by solubilization inside the micelles. For $d_2$−FA solubilized in the micelles, we observe modest 10−20 $cm^{-1}$ shifts to higher frequency. If hydrogen bonding were eliminated or considerably reduced as it is hypothesized for water inside AOT reverse micelles,[4−9,11] then the observed shifts should be at least 100 $cm^{-1}$ based on the reported values for $d_2$−FA in a Xe matrix.[47] These minor shifts indicate that the $d_2$−FA molecules inside the AOT reverse micelles retain a substantial degree of hydrogen bonding and that the bond lengths and angles are not strongly perturbed from their values in bulk even for the smallest micelles investigated, $w_{FA} = 0.5$.

Second, the relative amplitudes of the $ND_2$ modes increase with increasing $w_{FA}$. This trend is similar to what is observed for water and $D_2O$ inside AOT reverse micelles.[4−9] The amplitudes of the frequency components associated with the strongly hydrogen-bonded $ND_2$ stretching modes increases solvent loading without a significant change in frequency. This supports the interpretation that the formamide inside even the smallest micelles probed, $w_{FA} = 0.5$, forms hydrogen bonds that are much like those found in bulk $d_2$−FA.

Third, while the $ND_2$ stretching frequencies shift from higher to lower frequency as $w_{FA}$ increases, these shifts are substantially smaller than the shifts seen for water.[4,6,7] This suggests a similar degree of hydrogen bonding for the sequestered $d_2$−FA in all sizes of micelles measured.

In contrast, the water environment in AOT reverse micelles possesses little hydrogen bonding at the same $w$ values as those measured here and only develops substantial hydrogen-bonding character for significantly larger micelles. When water or $D_2O$ is solubilized inside AOT micelles in similar amounts as the $d_2$−FA in this study, that is, $w_0 = 2.0$, spectral shifts = 100 $cm^{-1}$ result.[5−7,9] This can be seen in the OD stretching region of $D_2O$ solubilized in AOT reverse micelles spectra shown in Figure 3b. These spectra reveal that a substantial fraction of the hydrogen bonding normally found in water is destroyed in the AOT reverse micelles. Several studies have proposed that ~3−4 water molecules can be strongly bound to each AOT headgroup.[6,9,10] Following the OH stretching modes, Amico et al.[6] find that only at water content $w_0 > 3$ do the spectra indicate the presence of hydrogen-bonded water. Water binding to the surfactant headgroup is also borne out by IR spectra of the AOT.[9,10] Both Christopher et al.[9] and Moran et al.[10] have observed shifts associated with increasing water loading for the sulfonate moiety of the AOT headgroup that indicate 1−3 water molecules bridge between the sulfonate and the sodium counterion, with further water molecules forming a hydrogen-bonded water pool.

The C═O stretching region of the IR spectrum also supports the interpretation that FA retains hydrogen-bonding character and does not interact strongly with the AOT polar headgroup. While it is not as sensitive to hydrogen bonding as the $ND_2$ stretching modes, perturbations of the C═O frequency can be observed arising from dissimilar environments.[50,51] Three spectral components are evident in $d_2$−FA/AOT/$CCl_4$ spectra in the frequency range 1600−1800 $cm^{-1}$ shown in Figure 4. The peak near 1685 $cm^{-1}$ can be attributed to FA because the spectrum of dry AOT in $CCl_4$, Figure 4b, shows no peak in this spectral region,[61] and because the vibrational frequency of the C═O stretch in bulk $d_2$−FA appears at 1670 $cm^{-1}$.[45,46] The spectral peaks observed at 1729 and 1739 $cm^{-1}$ are near the C═O stretching mode of $d_2$−FA in a Xe matrix that peaks at 1732 $cm^{-1}$.[47] However, as the intensity of these peaks follows the AOT concentration rather than the $d_2$−FA concentration and feature at 1723 and 1735 $cm^{-1}$ are reported for AOT, they are undoubtedly due to the C═O stretching modes of the AOT succinate groups. While the C═O stretching frequency of $d_2$−FA in the AOT reverse micelles remains blue shifted from the value in bulk liquid, these spectra show that the hydrogen bonding of the C═O group is still significant inside the micelles. This is consistent with the observations made for the $ND_2$ stretching region. The frequencies of the C═O stretching modes due to the AOT succinate groups remain constant for all the samples. This indicates that neither the $d_2$−FA nor the $D_2O$ interacts strongly with the AOT succinate groups. Rather, the solvents are solubilized more centrally within the micelles.

The fact that the $d_2$−FA appears to retain a significant degree of hydrogen bonding within the micelles leads us to hypothesize

that its structure differs significantly from intramicellar water. In particular, we believe that the $d_2$−FA may not bridge between the sulfonate and sodium cation as water reportedly does.[9,10] Further studies probing the sulfonate vibrational modes could clarify this interpretation.

Recently, two separate groups have used FTIR spectroscopy to probe reverse microemulsions in nonpolar solvents with nonaqueous polar solvents using FTIR spectroscopy.[33,34,43] Shchipunov and Shumilina[33,34] investigated lecithin microemulsions with various nonaqueous polar solvents including formamide. These studies concentrated on how the different solvents, perturbed lecithin organogel formation and did not explore how the microemulsions perturbed the sequestered solvents. Arcoleo et al.[43] explored a range of physicochemical properties of AOT microemulsions with formamide and *n*-methylformamide (NMF) in heptane. In these studies, FTIR spectra showed that the FA remained invariant with changing volume fraction but varied with the amount of sequestered solvent, $w_{FA}$. They did not make any assignments to the bands observed stating only that a two-state bound and free model for the solvent was apparently too simplistic. However, there are some parallels between their spectra and ours. Specifically, the formamide spectra of Arcoleo et al. show relatively minor differences between the bulk liquid and that of the solvent inside the micelles. Indeed, the most significant difference appears to be increasing narrowing of the spectral features for the solvent inside progressively smaller the micelles. Spectral narrowing can indicate longer lifetimes or reduced inhomogeneity in the sample. Our spectra, if anything, show spectral narrowing as *more* $d_2$−FA is added. Their NMF and FA IR spectra show considerably more spectral changes with increasing solvent loading. However, it is difficult to compare the spectra as they are normalized using the most intense formamide peak. Finally, the AOT used in these experiments was used as received from the supplier meaning that it most likely contained some water in addition to the nonaqueous polar solvents added.

**Solvation Dynamics.** Our solvation dynamics experiments show that solvation dynamics for FA inside the AOT reverse micelles differs to a large extent from bulk FA solvent motion. While 20% of the solvent relaxation of the intramicellar FA does occur on an ultrafast time scale similar to bulk formamide, this component corresponds to a mere 10 $cm^{-1}$ relaxation. In comparison with the bulk dynamics, this component is not only slower, 0.5 ps vs 0.11 ps but also of substantially reduced amplitude. Therefore, our overall interpretation is that the solvent is essentially immobilized inside the reverse micelles. These results agree well with our results for water motion in AOT reverse micelles.[16,17] Water in very small reverse micelles also displays virtually no motion on the time scale of the experiment. As the reverse micelles swell, the water exhibits increased mobility. For the FA reverse micelles, the micelles do not solubilize sufficient solvent to develop a significant solvent pool. This makes it impossible to increase the micellar size sufficiently to observe a significant increase the solvent motion.[30]

The location of the probe molecule within the reverse micelles could disproportionately reflect certain solvent configurations. While the exact position of the C343 within the micelles is unknown, we are confident that the dynamics we measure arise from motion on the micellar interior because the dye is insoluble in the nonpolar phase. We have measured the time-resolved anisotropy in water/AOT/isooctane reverse micelles to investigate where the dye resides, that is, intercalated in the micellar interface, near the surface or in the interior water pool. Results from these experiments showed that it in micelles both with $w_0 = 1.1$ and 7.5, the dye is strongly associated with the micellar surface.[16] However, there is a small component of dye that appears to reside in the interior solvent pool, removed from the micellar interface. This implies that the dye does not act as a cosurfactant, inserting itself into the micellar interface. Rather, it resides in a more physisorbed state at the interface. Because C343 is more soluble in FA than it is in water, and by direct comparison with aqueous AOT reverse micelles, the C343 molecules in FA/AOT reverse micelles likely reside near but not intercalated into the micellar interface.

While the size of the formamide containing reverse micelles for the same *w* value are slightly larger than micelles containing water, this does not necessarily imply that the dye molecule will be removed from the surface. But it is also possible that the dye resides further from the micellar interface in the FA/AOT/isooctane micelles than it does in water containing reverse micelles and that this leads to the small ultrafast component observed for the FA inside the micelles. However, the dominant dynamical response occurring on the hundreds of picosecond time scale and the minute Stokes shift indicates that the intramicellar FA differs greatly from bulk FA; the solvent is unable to move freely inside the reverse micelles.

**Interplay of Vibrations and Solvation Dynamics.** Before comparing results from the two experiments, we must consider how the differences in the samples used for the two techniques affect the results. First, we have reported the solvation dynamics of protonated FA, while $d_2$−FA was used in the IR experiments. The effect of deuteration on the FA dynamics has been measured via ultrafast time-resolved optical Kerr effect experiments.[53] These studies showed that both the inertial and the diffusive motion of FA were slowed when hydrogen was replaced with deuterium. The magnitude of the effect was consistent with the change in the molecular moments of inertia. Therefore, for the experiments reported here, the dynamics that would be observed for $d_2$−FA inside the reverse micelles would be slower than those for protonated FA. Since the FA inside the reverse micelles appears largely immobilized on the time scale of these experiments, the exchange of D for H would not change the observed dynamics to a large degree. Finally, we reiterate that the IR spectra of protonated FA in the reverse micelles show similar trends to the trends seen for $d_2$−FA.

The other difference between the systems probed with vibrational spectroscopy and solvation dynamics is the continuous nonpolar phase in which the reverse micelles formed. Vibrational spectra were measured in $CCl_4$, while solvation dynamics were measured in isooctane. The interaction of the nonpolar solvent with the surfactant tails can influence the size of the reverse micelles formed. The aggregation number for aqueous AOT reverse micelles in $CCl_4$ is smaller than it is for alkanes, 14−17 versus 20−23.[2] However, our DLS measurements, given in Table 1, indicate that the micelles formed in isooctane and $CCl_4$ are essentially the same size. A comparison of water/AOT/alkane and water/AOT/$CCl_4$ IR spectra show that the water vibrations are unaffected by the oil phase in these systems.[6] Furthermore, the overall results observed for FA/AOT/alkane reverse micelles, studied by Arcoleo et al.,[43] show similar trends for the intramicellar FA as those of our results for $d_2$−FA/AOT/$CCl_4$ and FA/AOT/$CCl_4$. Therefore, we believe that while the oil can have a strong influence on the nature of the nonpolar tails in solution, it does not significantly affect the intramicellar FA pool. Thus, the probed FA environments are essentially the same.

In these experiments, we anticipated that IR spectroscopy and

solvation dynamics data would provide complimentary information about the intramicellar FA. Steady-state spectral measurements are commonly used to predict the dynamical nature of a system. In homogeneous environments, this can sometimes be warranted. However, IR spectroscopy used to define molecular characteristics in heterogeneous environments can be dangerous and lead to faulty conclusions, as shown by the results reported here. The vibrational motion insinuates that the FA sequestered inside the micelle has structural features very similar to bulk liquid. This could lead one to predict that other molecular motions, such as translations and rotations, for molecules in the reverse micelles should also be similar to bulk liquid; indeed, this type of generalization is common. However, the solvation dynamics measurements show that the FA translational and rotational motion is highly restricted, essentially frozen in the reverse micelles. For intramicellar water, the vibrational modes are significantly perturbed, thus we expect other dynamics to be significantly perturbed.

The solvation dynamics of FA in the reverse micelles suggest that the vibrational spectrum should be comparable to solid FA. When a liquid solidifies, the translational and rotational degrees of freedom are reduced, while vibrational modes may not be substantially altered.[62] This is usually accompanied by a sharpening of the vibrational features due to increased sample homogeneity and longer lifetimes for molecular states. However, the IR spectral features for intramicellar $d_2$−FA are broader than the corresponding features in the bulk liquid, while the solvation dynamics are slower for FA inside the micelles. These two results do not follow the normal trend for liquids immobilized by solidification. In contrast, it may reflect a high degree of inhomogeneity for solvent inside the micelles.

In a study related to this work, we have investigated the dynamics of polar solvation for water in lecithin/cyclohexane reverse micelles.[63] In that study, we found the interpretation that bulklike, hydrogen-bonded water exists in the microheterogeneous solution, both from the vibrational (IR and Raman) spectra and NMR studies,[64−67] were not supported by the water solvation dynamics we measured. Our results indicated that water was strongly bound to the lipid interface and largely immobilized even though the vibrations of the water showed hydrogen-bonding characteristics. These results support the results reported here and show that it is dangerous to interpret the dynamical nature of a system without a full investigation of the various possible molecular motions.

## Summary

In this paper, we report on the IR vibrational spectroscopy and time-resolved solvation dynamics of formamide in the restricted environment of an Aerosol OT reverse micelle. Vibrational spectra of this highly structured, hydrogen-bonded solvent in reverse micelles appear almost unchanged from the bulk liquid spectrum. In comparison, water in similar reverse micellar milieus shows significant spectral shifts indicative of reduced hydrogen bonding. The solvation dynamics of both water and formamide in these reverse micelles reveals that characteristic bulk solvent motion is virtually absent. This result is predicted for water, whose structure implied from vibrational spectroscopy departs from bulk. However, if the vibrational motion for formamide in reverse micelles is used as a general predictor of the "nature" of the solvent, then the solvation dynamics provide a striking contrast. The implications of this result are far reaching for molecules in heterogeneous environments. These results show that steady-state spectroscopy may not always be a good predictor for dynamical behavior.

**Acknowledgment.** This work was supported by the National Science Foundation and Colorado State University. We are very grateful to Professor Ellen R. Fisher for allowing us to use her FTIR spectrometer. N.E.L. is the recipient of a NSF Young Investigator award. E.P.U. and J.R.K. are undergraduate research assistants.

## References and Notes

(1) Jones, M. N.; Chapman, D. *Micelles, Monolayers, and Biomembranes*; John Wiley and Sons: New York, 1995.
(2) De, T.; Maitra, A. *Adv. Colloid Interface Sci.* **1995**, *59*, 95.
(3) Zulauf, M.; Eicke, H.-F. *J. Phys. Chem.* **1979**, *83*, 480.
(4) Onori, G.; Santucci, A. *J. Phys. Chem.* **1993**, *97*, 5430.
(5) Zhukovskii, A. P.; Petrov, L. N.; Rovnov, N. V. *Zh. Strukt. Khim.* **1991**, *32*, 81.
(6) Amico, P.; D'Angelo, M.; Onori, G.; Santucci, A. *Il Nuovo Cimento* **1995**, *17*, 1053.
(7) D'Angelo, M.; Fuccello, A.; Onori, G.; Santucci, A. *Prog. Colloid. Polym. Sci.* **1993**, *93*, 350.
(8) D'Aprano, A.; Lizzio, A.; Turco Liveri, V.; Aliotta, F.; Vasi, C.; Migliardo, P. *J. Phys. Chem.* **1988**, *92*, 4436.
(9) Christopher, D. J.; Yarwood, J.; Belton, P. S.; Hills, B. P. *J. Colloid Interface Sci.* **1992**, *152*, 465.
(10) Moran, P. D.; Bowmaker, G. A.; Cooney, R. P. *Langmuir* **1995**, *11*, 738.
(11) Jain, T. K.; Varshey, M.; Maitra, A. *J. Phys. Chem.* **1989**, *93*, 7409.
(12) Hasegawa, M.; Sugimura, T.; Shindo, Y.; Kitahara, A. *Colloids Surf. A* **1996**, *109*, 305.
(13) Zhang, J.; Bright, F. V. *J. Phys. Chem.* **1991**, *95*, 7900.
(14) Cho, C. H.; Chung, M.; Lee, J.; Nguyen, T.; Singh, S.; Vedamuthu, M.; Yao, S. H.; Zhu, J. B.; Robinson, G. W. *J. Phys. Chem.* **1995**, *99*, 7806.
(15) Sarkar, N.; Das, K.; Datta, A.; Das, S.; Bhattacharyya, K. *J. Phys. Chem.* **1996**, *100*, 10523.
(16) Riter, R. E.; Willard, D. M.; Levinger, N. E. *J. Phys. Chem. B* **1998**, *102*, 2705.
(17) Riter, R. E.; Undiks, E. P.; Levinger, N. E. *J. Am. Chem. Soc.* **1998**, *120*, 6062.
(18) Mittleman, D. M.; Nuss, M. C.; Colvin, V. L. *Chem. Phys. Lett.* **1997**, *275*, 332.
(19) Jimenez, R.; Fleming, G. R.; Kumar, P. V.; Maroncelli, M. *Nature* **1994**, *369*, 471.
(20) Barbara, P. F.; Jarzeba, W. In *Advances in Photochemistry*; Volman, D. H., Hammond, G. S., Gollnick, K., Eds.; John Wiley & Sons: New York, 1990; Vol. 15, p 1.
(21) Maroncelli, M.; MacInnis, J.; Fleming, G. R. *Science* **1989**, *243*, 1674.
(22) Maroncelli, M. *J. Mol. Liq.* **1993**, *57*, 1.
(23) Horng, M. L.; Gardecki, J. A.; Papazyan, A.; Maroncelli, M. *J. Phys. Chem.* **1995**, *99*, 17311.
(24) Kahlow, M. A.; Jarzeba, W.; Kang, T. J.; Barbara, P. F. *J. Chem. Phys.* **1989**, *90*, 151.
(25) Castner Jr., E. W.; Maroncelli, M.; Fleming, G. R. *J. Chem. Phys.* **1987**, *86*, 1090.
(26) Bessho, K.; Uchida, T.; Yamauchi, A.; Shioya, T.; Teramae, N. *Chem. Phys. Lett.* **1997**, *264*, 381.
(27) Yanagimachi, M.; Tamai, N.; Masuhara, H. *Chem. Phys. Lett.* **1992**, *200*, 469.
(28) Vajda, S.; Jimenez, R.; Rosenthal, S. J.; Fidler, V.; Fleming, G. R.; Castner, E. W., Jr. *J. Chem. Soc., Faraday Trans.* **1995**, *91*, 867.
(29) The distinction between reverse micelles and reverse microemulsions is often ill defined. For this work, we use the convention given by De and Maitra (ref 2) defining reverse microemulsions as solutions containing a ternary or higher order mixture that display a single phase. We define reverse micelles as noncontinuous, noninteracting aggregates of surfactant molecules that delineate a polar phase from a nonpolar phase.
(30) Riter, R. E.; Kimmel, J. R.; Undiks, E. P.; Levinger, N. E. *J. Phys. Chem. B* **1997**, *101*, 8292.
(31) Rico, I.; Lattes, A. In *Microemulsion Systems*; Rosano, H. L., Clausse, M., Eds.; Marcel Dekker: 1987; Vol. vol 24.
(32) Rico, I.; Lattes, A. In *Microemulsion Systems*; Rosano, H. L., Clausse, M., Eds.; Marcel Dekker: New York, 1987; Vol. 24.
(33) Shchipunov, Y. A.; Shumilina, E. V. *Mater. Sci. Eng. C* **1995**, *3*, 43.
(34) Shchipunov, Y. A.; Shumilina, E. V. *Colloid J.* **1996**, *58*, 123.
(35) Ray, S.; Moulik, S. P. *Langmuir* **1994**, *10*, 2511.
(36) Friberg, S. E.; Rong, G.; Ward, A. J. I. *J. Phys. Chem.* **1988**, *92*, 7247.
(37) Mathew, C.; Saidi, Z.; Peyrelasse, J.; Boned, C. *Phys. Rev. A* **1991**, *43*, 873.

(38) Gautier, M.; Rico, I.; Ahmad-Zadeh Samii, A.; De Savignac, A.; Lattes, A. *J. Colloids Interface Sci.* **1986**, *112*, 484.
(39) Friberg, E.; Podzimek, M. *Colloid Polym. Sci.* **1984**, *262*, 252.
(40) Ahamd-Zadeh Samii, A.; de Savignac, A.; Rico, I.; Lattes, A. *Tetrahedron* **1985**, *41*, 3683.
(41) Chhabra, V.; Lal, M.; Maitra, A. N. *J. Mater. Res.* **1995**, *10*, 2689.
(42) Mukherjee, L.; Mitra, N.; Bhattacharya, P. K.; Moulik, S. P. *Langmuir* **1995**, *11*, 2866.
(43) Arcoleo, V.; Aliotta, F.; Goffredi, M.; La Manna, G.; Turco Liveri, V. *Mater. Sci. Eng. C* **1997**, *5*, 47.
(44) Camardo, M.; DAngelo, M.; Mannaioli, S.; Onori, G.; Santucci, A. *Colloid Surf. A* **1996**, *119*, 183.
(45) Suzuki, I. *Bull. Chem. Soc. Jpn.* **1960**, *33*, 1359.
(46) Gardiner, D. J.; Lees, A. J.; Straghan, B. P. *J. Mol. Struct.* **1979**, *53*, 15.
(47) Rasanen, M. *J. Mol. Struct.* **1983**, *101*, 275.
(48) Sugawara, M.; Fujimura, Y. *J. Chem. Phys.* **1994**, *101*, 6586.
(49) Ganeshsrinivas, E.; Sathyanarayana, D. N.; Machida, K.; Miwa, Y. *J. Mol. Struct.* **1997**, *403*, 153.
(50) Lees, A. J.; Straughan, B. P.; Gardiner, D. J. *J. Mol. Struct.* **1979**, *54*, 37.
(51) Bukowska, J. *J. Mol. Struct.* **1983**, *98*, 1.
(52) Lee, Y.-T. *J. Raman Spectrosc.* **1997**, *28*, 45.
(53) Chang, Y. J.; Castner, E. W., Jr. *J. Phys. Chem.* **1994**, *98*, 9712.
(54) Chang, Y. J.; Castner, E. W., Jr. *J. Chem. Phys.* **1993**, *99*, 113.
(55) This corresponds to fewer than one water molecule per micelle at the *w* values studied.
(56) Hilfiker, R.; Eicke, H. F.; Sager, W.; Steeb, C.; Hofmeier, U.; Gehrke, R. *Ber. Bunsen-Ges. Phys. Chem.* **1990**, *94*, 677.
(57) Brucker, G. A.; Kelley, D. F. *J. Phys. Chem.* **1987**, *91*, 2856.
(58) Parsapour, F.; Kelley, D. F. *J. Phys. Chem.* **1996**, *100*, 2791.
(59) Bukowska, J. *Spectrochim. Acta* **1979**, *35A*, 985.
(60) *Water: A Comprehensive Treatise*; Franks, F., Eds.; Plenum Press: New York, 1972; Vol. 1.
(61) Moran, P. D.; Bowmaker, G. A.; Cooney, R. P.; Bartlett, J. R.; Woolfrey, J. L. *J. Mater. Chem.* **1995**, *5*, 295.
(62) Herzberg, G. H. *Molecular Spectra and Molecular Structure II. Infrared and Raman Spectra of Polyatomic Molecules*; Krieger: Malabar, FL, 1991 (reprint).
(63) Willard, D. M.; Riter, R. E.; Levinger, N. E. *J. Am. Chem. Soc.* **1998**, *120*, 4151.
(64) Capitani, D.; Segre, A. L.; Sparapani, R. *Langmuir* **1991**, *7*, 250.
(65) Capitani, D.; Rossi, E.; Segre, A. L.; Giustini, M.; Luisi, P. L. *Langmuir* **1993**, *9*, 685.
(66) Cavallaro, G.; La Manna, G.; Turco Liveri, V.; Aliotta, F.; Fontanella, M. E. *J. Colloid Inter. Sci.* **1995**, *176*, 281.
(67) Maitra, A.; Jain, T. K.; Shervani, Z. *Colloid Surf.* **1990**, *47*, 255.
(68) Riddick, J. A.; Bunger, W. B.; Sakano, T. K. *Organic Solvents*, 4 ed.; John Wiley and Sons: New York, 1986; Vol. II.